The role of contact size on the formation of Schottky barriers and ohmic contacts at nanoscale metal-semiconductor interfaces

R. A. Kraya[1,a)] and L. Y. Kraya[2]
[1]*Department of Materials Science and Engineering, University of Pennsylvania, Philadelphia, Pennsylvania 19104, USA*
[2]*Department of Electrical Engineering, Princeton University, Princeton, New Jersey 08544 USA*

(Received 25 September 2011; accepted 16 February 2012; published online 16 March 2012)

We have measured the electronic structure at Au nanoisland–niobium doped $SrTiO_3$ interfaces over a range of contact diameters. Electron transport processes at the interface transition from thermionic emission dominated to tunneling dominated, leading to ohmic behavior at small sizes. The transition increases at a much higher rate than is generally expected, emphasizing the need for precise control of nanoscale dimensions for reproducible effects in nanoscale electronic devices. © *2012 American Institute of Physics*. [http://dx.doi.org/10.1063/1.3693542]

I. INTRODUCTION

The transition to the "nanoelectronics age" will require an understanding of how downscaling device dimensions to the nanometer regime will affect functionality and will require the creative manipulation of these characteristics to create novel and revolutionary advancements in technology. Electrical control at metal-semiconductor (ms) interfaces is a fundamental advancement needed at the nanoscale with further research necessary to understand the fundamental mechanisms of current transport across the interface. Our current understanding of the mechanisms of interface barrier formation has not progressed further than an elementary level.[1] Recent theoretical and experimental work has shown a size dependence of the interface to transport with increased tunneling contributions as the size decreases.[2–10]

Many theories have been proposed to describe charge transport at millisecond interfaces. Early models on macroscopic contacts described transport as either dominated by thermionic processes or tunneling process primarily dependent on the dopant concentration in the semiconductor.[11] Modern theory has shown that as contact size decreases the transport becomes more tunneling dominant, independent of the dopant concentration.[2–4] However, it is not always entirely clear how much a small change can affect transport properties. This information is especially important for understanding resistive switching phenomena this is an attractive option for future memory devices. There are more than a dozen mechanisms[12–14] that can be used to explain resistive switching effects including electrostatic and electronic effects at the interface between the metal contact and switching material. Testing nanoscale theories of charge transport requires well defined contact sizes with the metal annealed to the semiconductor surface. All contacts would ideally be located on a single surface to ensure similarly defined interfaces.

In this work, conductive atomic force microscopy (cAFM) is used to explore these issues at nanoscale Au–$SrTiO_3$ interfaces. $SrTiO_3$ is the prototypical metal oxide material. With a bandgap of 3.2 eV and a dielectric constant of $\sim 300\varepsilon_0$,[15] $SrTiO_3$ is a semiconducting oxide material and behaves as an n-type semiconductor when doped with niobium.

II. EXPERIMENTAL SETUP

Here single-side epitaxially polished Nb-doped (0.02 at. % Nb) $SrTiO_3$ (100) were rinsed with acetone and ethanol and air dried with nitrogen. The substrates were then annealed inflowing hydrogen for 1 h at 900 °C, leading to reduced substrates as opposed to oxidized substrates in previous publications.[6–10] The reduced Nb-doped substrates were contacted to Au metal nanoparticles from solutions of 20, 50, and 100 nm sizes.[16] This was followed by a subsequent annealing inflowing hydrogen. (Fig. 1) The samples were ground to gold coated pucks using silver paint. Contacts to the nanoparticles were made with a Pt/Ir coated AFM tip with a nominal force of 60 nN. Current was measured as function of applied bias for single contacts between 30 and 60 nm in diameter. The interface size was estimated to be the full width at half maximum (FWHM) height for the nanoparticles measured.

The largest contacts [1, 58 nm FWHM (red, A), and 2, 52 nm FWHM (green, B)] (Fig. 2) showed clear bias dependent resistance. For contact 2, the dependence is reduced. Another diameter reduction of 8 nm (44 nm diameter: blue) led to ohmic behavior with a linear relationship observed between the current and voltage. Decreasing the contact size further led to *I-V* curves that looked completely vertical on a scale of tenths of volts, making immediate comparisons of the nanointerfaces difficult. The curves were subsequently expanded to compare the findings for nanoparticles less than 40 nm in diameter.

The nanointerfaces exhibiting bias dependent behavior were plotted on a $\log(I/E^2)$ versus $1/E$ and found to be linear, indicating transport by Fowler–Nordheim (FN) tunneling through a triangular potential barrier as a viable mechanism of charge transport through the interface. The FN tunneling equation is the following:[17,18]

a)Author to whom correspondence should be addressed. Electronic mail: ramsey.kraya@gmail.com.

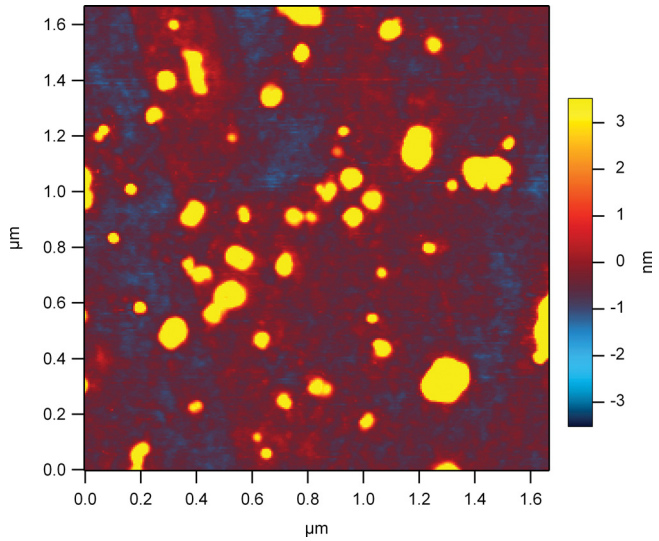

FIG. 1. (Color online) AFM topography image of a reduced Nb doped $SrTiO_3$ substrate contacted by gold nanoparticles.

$$J = (A/\phi_B) \times \mathrm{E}^2 \exp\left(-\mathrm{B}\frac{\phi_\mathrm{B}^{3/2}}{\mathrm{E}}\right), \tag{1}$$

$$A = \frac{e^3 m_{Au}}{8\pi h m_{SrTiO_3}}, \tag{2}$$

$$B = \frac{8\pi\sqrt{2m_{SrTiO_3}}}{3he} = 6.83 \times 10^7 \sqrt{m_{SrTiO_3}/m_{Au}}, \tag{3}$$

$$E = \sqrt{\frac{2N_d eV}{\varepsilon\varepsilon_o}} = 0.1902\sqrt{\frac{N_d V}{\varepsilon}}, \tag{4}$$

where J is the current density, E is the electric field at the interface, A and B are constants, A_{eff} is the effective tunneling area, m_{Au} is the effective mass of the gold nanoparticle $\sim m_e$, the mass of an electron and m_{srtio3} is $\sim 1.8\ m_e$, e is the electron charge, h is Plank's constant, ϕ_B is the barrier height, V is the applied potential, N_d is the dopant concentration, ε is the relative permittivity of $SrTiO_3$, and ε_o is the permittivity of free space. The equation was fit to the transport data of the two largest contacts (58 and 52 nm) to determine the barrier height (Figs. 3(a) and 3(b)). The barrier height was calculated to be 0.69 eV and 0.42 eV, respectively. Large values of A indicated that F-N tunneling was not the most appropriate method for characterizing the interfaces. However, a decreasing value of A would indicate a trend to increased tunneling transport processes with decreasing contact size.[19]

The nanointerfaces were then plotted on a logarithmic plot and fit to the thermionic emission equation:

$$I = I_s \exp\left(\frac{eV_D}{nk_BT}\right)\left[1 - \exp\left(\frac{eV_D}{k_BT}\right)\right], \tag{5}$$

$$I_s = Area * A^{**}T^2 \exp\left(-\frac{e\Phi^{eff}}{kT}\right), \tag{6}$$

$$A^{**} = 4\pi m^* k^2/h^3, \tag{7}$$

where $Area$ is the contact area, A^{**} is the Richardson constant, k_B is Boltzmann constant, T is temperature, eV_D is the applied voltage, I is the current, Φ^{eff} is the Schottky barrier

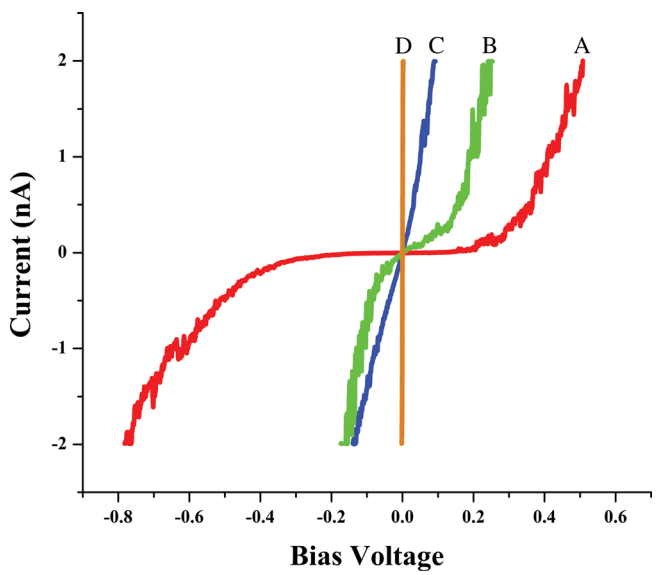

FIG. 2. (Color online) Current–voltage characteristics at Au nanoparticle reduced Nb doped interfaces of varying diameters: red (A), 58 nm; green (B), 52 nm; blue (C), 45 nm; gold (D), 37 nm.

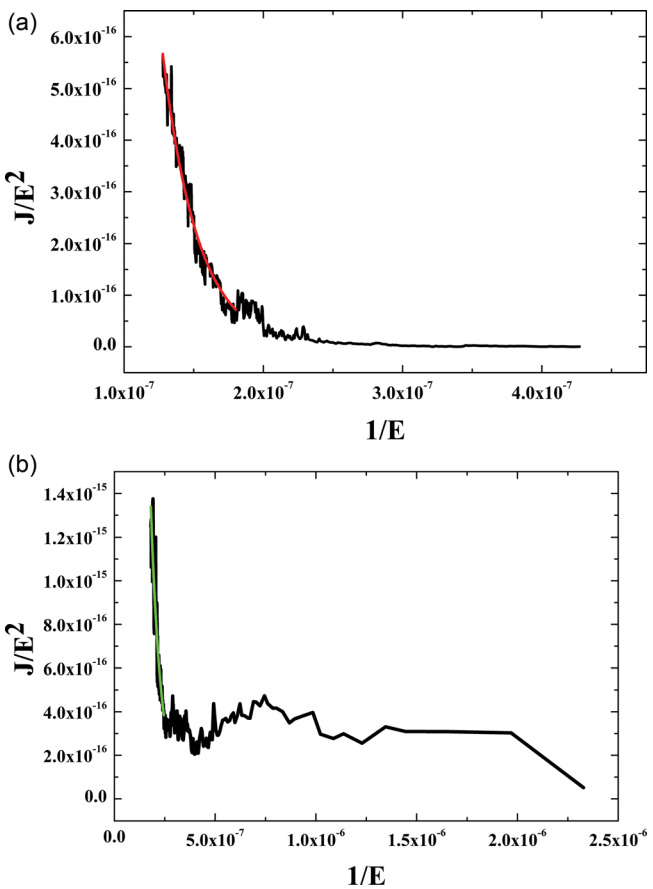

FIG. 3. (Color online) Variation of the current divided by the square of the electric field with the inverse electric field for 58 nm (a) and 52 nm (b) contact. Fowler-Norheim tunneling injection theory predicts $I/E^2 \propto -1/E$. Best fit lines with data are shown. Barrier heights are 0.69 eV and 0.43 eV and A is 5.92×10^{-14} and 1.8×10^{-14} for (a) and (b), respectively. The carrier concentration was measured to be $3 \times 10^{19}\mathrm{cm}^{-3}$ for the sample.

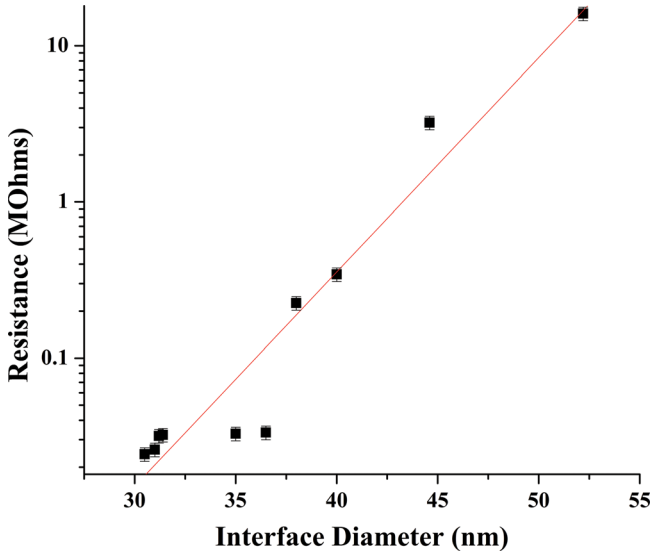

FIG. 4. (Color online) Contact resistance vs diameter for the measured Nb doped $SrTiO_3$ interfaces. The data follow a straight line path on a log scale with contact resistance increasing with increasing interface size.

height (SBH), I_s is the saturation current density, and n is the ideality factor.

Equation 1 was fit to the transport data of the two largest contacts (58 and 52 nm) to determine the barrier height and ideality factor. The SBH was calculated to be 0.59 eV with an ideality factor of $n = 1.17$. For the second largest interface (52 nm), the barrier height was calculated to be 0.41 eV with $n = 2.63$. Next, the contact resistance was determined for all contacts below 55 nm. The contact resistance is defined as

$$R_c \equiv \left(\frac{dJ}{dV_D}\right)^{-1}_{V_D=0}, \tag{8}$$

where R_c is the contact resistance.[11] Plotting interface size versus contact resistance on a log scale (Fig. 4) reveals an exponential dependence of the contact resistance on the contact size in the nanometer regime. A decrease in the contact resistance of over 3 orders of magnitude was observed for a change in interface size of less than 20 nm.

III. RESULTS AND DISCUSSION

An analysis of the results reveals a number of important characteristics. The SBH on the largest contact is considerably lower than for those reported on oxidized surfaces and is in line with the work of Copel *et al.*[20] and Chung *et al.*,[21] who observed lower values for the barrier height at reduced $SrTiO_3$ contacts to platinum. For contact 2, with a diameter 6 nm smaller than contact 1, the ideality factor increases to a value greater than 2, indicating a transition from thermionic emission to tunneling as the dominant transport mechanism. This is due to the increased contributions of the edges to the overall transport processes as the size of the contact is reduced. At the edges of the interface, the electric field is greater than in the bulk. The boundaries of the interfaces are known to exhibit increased electric field intensities with a higher a radius of curvature experiencing greater intensity.[22–26] Therefore the electric field, and thus band bending, will be great at the edges of the interface, while at the center of the interface the electric field should be similar to that of an infinite plain of charge. Greater band bending at the edges combined with an increasing contribution of the edges to the overall transport processes results in increased charge flow through the interface as the size decreases. Pomarico *et al.*[5] utilized cAFM techniques to simultaneously map the topography and current of the samples, revealing enhanced conductivity at the edges of the nanostructures. Smit *et al.*[2–4] have shown computationally that the ratio of tunneling to thermionic emission at metal semiconductor (ms) interfaces will increase as the diode size decreases.

As the interface sizes continued to decrease, a transition occurred from a tunnel contact to an ohmic contact behavior where resistance is independent of applied bias. Decreasing the interface size further revealed an exponential relationship between size and conductivity. The implications are that small variations (in the single nanometer range) in contact size can have dramatic effects on interface dynamics and that precise control of the interface size is imperative for reproducible effects in nanodevices.

IV. CONCLUSION

In conclusion, the transport characteristics of reduced oxide metal nanoparticle interfaces were studied using conductive atomic force microscopy. The local *I-V* characteristics over a range of sizes revealed a transition from thermionic to tunneling to ohmic interfaces with the conductivity increasing exponentially with a linear decrease in contact size. These findings highlight the relevance and sensitivity of the electrostatic and electronics effects to variations in contact size. For the future, varying the contact size at the interface can be used to understand resistive switching mechanisms and the effects of ohmic and tunnel contacts to switching phenomena.

ACKNOWLEDGMENTS

This research was supported by the U.S. Department of Energy under Grant DE-FG02–00ER45813-A000 and by the National Science Foundation IGERT Program DGE02–21664; facilities use in the Laboratory for Research on the Structure of Matter (DMR05–20020) are gratefully acknowledged.

[1]R. T. Tung, Mater. Sci. Eng. R. **35**, 1 (2001).
[2]G. D. J. Smit, S. Rogge, and T. M. Klapwijk, Appl. Phys. Lett. **80**, 2568 (2002).
[3]G. D. J. Smit, M. G. Flokstra, S. Rogge, and T. M. Klapwijk, Microelectr. Eng. **64**, 429 (2002).
[4]G. D. J. Smit, S. Rogge, and T. M. Klapwijk, Appl. Phys. Lett. **81**, 3852 (2002).
[5]A. A. Pomarico, D. Huang, J. Dickinson, A. A. Baski, R. Cingolani, H. Morkoc, and R. Molnar, Appl. Phys. Lett. **82**, 1890 (2003).
[6]R. A. Kraya and L. Y. Kraya, IEEE Trans. Nanotechnol. **11**, 3 (2012).
[7]L. Y. Kraya and R. Kraya, J. Appl. Phys. **111**, 013708 (2012).
[8]R. A. Kraya and D. A. Bonnell, IEEE Trans. Nanotechnol. **9**, 741 (2010).
[9]R. Kraya, L. Y. Kraya, and D. A. Bonnell, Nano Lett. **10**, 1224 (2010).
[10]R. A. Kraya, Appl. Phys. Lett. **99**, 053107 (2011).
[11]M. Winfried, *Electron Properties of Semiconductors* (Springer-Verlag, New York, 2004).

[12]R. Waser, R. Dittmann, G. Staikov, and K. Szot, Adv. Mater. **21**, 2632 (2009).
[13]J. R. Contreras, H. Kohlstedt, U. Poppe, R. Waser, C. Buchal, and N. A. Pertsev, Appl. Phys. Lett. **83**, 4595 (2003).
[14]A. Sawa, Materials Today **11**, 28 (2008).
[15]K. Nassau and A. E. Miller, J. Cryst. Growth **91**, 373 (1988).
[16]K. Lee, M. Duchamp, G. Kulik, A. Magrez, J. W. Seo, S. Jeney, J. Kulik, and L. Forro, Appl. Phys. Lett. **91**, 173112 (2007).
[17]M. Ahrens, R. Merkle, B. Rahmati, and J. Maier, Physica B **393**, 239 (2007).
[18]A. J. Hartmann, R. N. Lamb, J. F. Scott, P. N. Johnston, M. El Bouanani, C. W. Chen, and J. Robertson, J. Korean Phys. Soc. **32**, S1329 (1998).
[19]A. J. Campbell, D. D. C. Bradley, and D. G. Lidzey, J. Appl. Phys. **82**, 6326 (1997).
[20]M. Copel, P. R. Duncombe, D. A. Neumayer, T. M. Shaw, and R. M. Tromp, Appl. Phys. Lett. **70**, 3227 (1997).
[21]Y. W. Chung and W. B. Weissbard, Phys. Rev. B **20**, 3456 (1979).
[22]R. T. Tung, *Contacts to Semiconductors* (Noyes, New York, 1993).
[23]R. T. Tung, Phys. Rev. B **45**, 13509 (1992).
[24]R. T. Tung, Phys. Rev. B **64**, 205310 (2001).
[25]J. D. Jackson, *Classical Electrodynamics*, 3rd ed. (Wiley and Sons, New York, 1999).
[26]P. A. Tove, J. Phys. D **15**, 517 (1982).